Equivalent linearization method improved by higher order statistics in modal space for geometrically nonlinear vibrations

Zhi Wang[a], Yahui Zhang[a*], David Kennedy[b]

[a] *State Key Laboratory of Structural Analysis for Industrial Equipment, Department of Engineering Mechanics, International Center for Computational Mechanics, Dalian University of Technology, Dalian 116023, PR China;*

[b] *School of Engineering, Cardiff University, Cardiff CF24 3AA, Wales, UK*

*Corresponding author:

Dr. Y. H. Zhang

State Key Laboratory of Structural Analysis for Industrial Equipment, Department of Engineering Mechanics, Dalian University of Technology, Dalian 116023, PR China

Email: zhangyh@dlut.edu.cn

Tel: +86 411 84706337

Fax: +86 411 84708393

Abstract

In this paper, an equivalent linearization method considering higher order statistics based on nonlinear reduced order modeling techniques is proposed for the geometrically nonlinear random vibration problems of complex structures. Nonlinear reduced order models of the structures are constructed by leveraging the nonlinear analysis capabilities of commercial finite element codes, and an improvement to the Stiffness Evaluation Procedure method for determining the stiffness coefficients is achieved through the equivalence relation, leading to a notable reduction in computational cost with no further requirements for commercial finite element codes. The nonlinear terms are twice regulated equivalent, and then a regulated form of the stiffness coefficients is derived to introduce higher order statistics into the equations of motion. Then a linearized system obtained by the criterion of force error minimization is used to predict the random response of the original nonlinear system. The nonlinear problems are solved by the linearized system in the modal space, increasing computational efficiency significantly. Higher order statistical information of the response is introduced to improve the accuracy. Typical examples are used to verify the effectiveness of the proposed method, while its applicability is further demonstrated via the analysis of turbulence-excited composite laminates.

Keywords: Geometric nonlinearity; Nonlinear reduced order model; Equivalent linearization; Turbulent boundary layer excitation; Higher order statistics

1 Introduction

In the process of high speed flight, components of aerospace vehicles are impacted by high intensity jets or turbulent boundary layers [1], resulting in severe vibration in which the geometrically nonlinear effects are significant and cannot be ignored. On the one hand, the severe vibration leads to fatigue damage to the structure and affects the service life of vehicles. On the other hand, it also has adverse effects on the operation of the vehicles, such as interference with the flight attitude or the normal operation of an attached pipeline.

Perturbation [2], the Fokker-Planck equation [3], [4], time-domain numerical simulation [5] -[7] and equivalent linearization (EL) [8], [9] are the main methods currently used to predict geometrically nonlinear random response [10]. The EL method equivalences the nonlinear system to a linear system by a linearization criterion, and then the mature linear random vibration method is applied to solve the nonlinear problem. This is the most popular among all approximation methods for the dynamics of a nonlinear system under random excitation [11], it can accurately capture response statistics over a wide range of response levels while maintaining a relatively light computational burden [12]. However, replacing the nonlinear terms by linear terms will yield some error and affect the computational accuracy [13]. In order to reduce the error, Anh and Di Paola [14] proposed a regulated equivalent linearization (REL) method, where the nonlinear terms are firstly equivalenced to higher order terms, and are then equivalenced to linear terms

in several steps. The REL method considers higher order statistics and can predict the motion behavior of the nonlinear system more accurately than the classical EL method. Elishakoff [13] further developed the REL method and applied it to a variety of single-degree-of-freedom systems, comparing with exact solutions and the results of the classical EL method. It was verified that the REL method has a notable advantage in accuracy. Subsequently, Anh and Elishakoff [15], [16] adopted the REL method to investigate the dynamic behavior of a Bernoulli-Euler beam and Seide's problem. The cost of the EL and REL methods is still unacceptable when applied to engineering structures with a considerable number of degrees of freedom.

Nonlinear reduced order modeling (NLROM) techniques reduce finite element models with a large number of degrees of freedom to a low order system of modal equations. Mignolet and Soize [17] gave a formula to directly determine the nonlinear stiffness coefficients in the reduced order models, but it requires specific finite element codes and is not conducive to complex structures. Rizzi and Muravyov [18] proposed a Stiffness Evaluation Procedure (STEP) method to indirectly determine the nonlinear stiffness coefficients by leveraging the nonlinear analysis capabilities of commercial finite element codes. This approach can easily reduce the order of complex structures. Muravyov and Rizzi [10] developed an EL method based on NLROM techniques, and successfully predicted the vibration response of a metal plate under band-limited white noise. This method is referred to as the NLROM-EL method in this paper. Yang and Yang

[19] investigated the random response of composite laminates under band-limited white noise using the NLROM-EL method. The reduced order modeling techniques reduce the order of the nonlinear system, and then the computational cost of response analysis is significantly reduced. In contrast, the cost of determining the nonlinear stiffness coefficients is more notable. Prerez et al. [20] developed an improved form of the method by using commercial finite element software that allows the output of tangent stiffness matrix, such as NASTRAN and ABAQUS, so reducing the cost.

The computational efficiency and accuracy should be considered comprehensively when solving geometrically nonlinear random vibration problems of complex engineering structures, at the same time, simulating the dynamics of a full finite element model using direct time integration presents a high computational cost [21]. This paper develops an EL method based on the NLROM and modified by higher order statistics. The EL and NLROM techniques effectively reduce the computational cost of predicting the geometrically nonlinear random response, while the higher order statistics improve the computational accuracy. Firstly, according to the nonlinear potential energy and nonlinear restoring force, the equivalent relationships between the stiffness coefficients are obtained, and the STEP method to determine the stiffness coefficients is optimized to construct reduced order models of the geometrically nonlinear structures with less cost. Then, referring to the REL method, the nonlinear terms of the reduced order equations of motion are twice regulated equivalent to derive a regulated form of the nonlinear stiffness

coefficients, so that the higher order statistics of the response can be introduced into the modal equations of motion. Finally, a linearized form of the nonlinear system is constructed by the criterion of force error minimization for the prediction of random response. Compared with the traditional EL method, the proposed method does not introduce new assumptions, so it keeps the same application scope as the former, that is, weakly nonlinear systems. The NLROM-EL method, time-domain numerical simulation and the proposed method are used to investigate a metal plate and a composite laminated plate under band-limited white noise in the literature. Considering that the turbulent boundary layer has a more complex expression in spatial correlation, the composite laminate under the turbulent boundary layer is further investigated. It is observed that the proposed method maintains the same iterative convergence and computational cost as the NLROM-EL method, but provides a significant improvement in computational accuracy over the NLROM-EL method for the same effort.

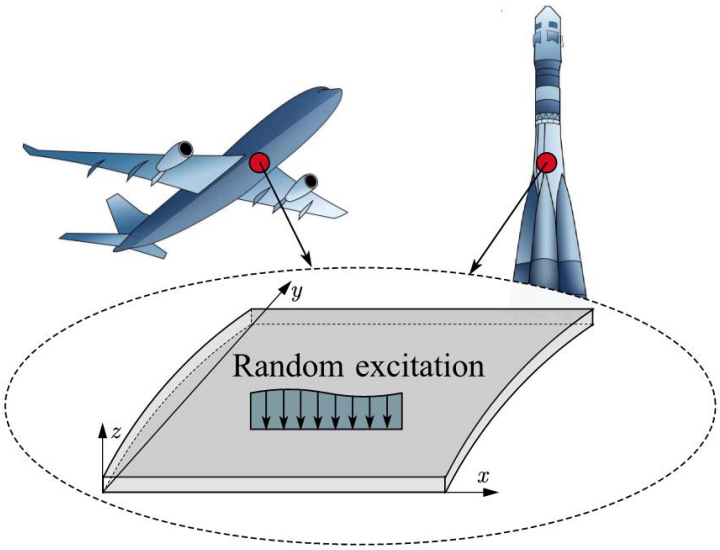

Fig. 1 Thin-walled structure subjected to random excitation

2 EL method for geometrically nonlinear structures

Thin-walled structures are common components in aerospace vehicles. When subjected to random excitation, as shown in Fig. 1, the geometrically nonlinear equations of motion for this kind of structure can be expressed as [12]

$$\boldsymbol{M}\ddot{\boldsymbol{X}} + \boldsymbol{C}\dot{\boldsymbol{X}} + \boldsymbol{K}\boldsymbol{X} + \boldsymbol{\Gamma}(\boldsymbol{X}^2, \boldsymbol{X}^3) = \boldsymbol{F} \tag{1}$$

where $\boldsymbol{M}, \boldsymbol{C}, \boldsymbol{K}$ are the mass, damping and linear stiffness matrices, respectively, $\boldsymbol{X}$ is the displacement response vector and $\boldsymbol{F}$ is the random excitation vector. $\boldsymbol{\Gamma}$ is the nonlinear restoring force vector which, when the material nonlinearity is not considered, can be expressed as a function of the quadratic and cubic terms of the displacement vector [12].

According to the EL method, an approximate solution to Eq. (1) can be obtained by an EL system [22]

$$\boldsymbol{M}\ddot{\boldsymbol{X}} + \boldsymbol{C}\dot{\boldsymbol{X}} + (\boldsymbol{K} + \boldsymbol{K}_{\mathrm{e}})\boldsymbol{X} = \boldsymbol{F} \tag{2}$$

where $\boldsymbol{K}_{\mathrm{e}}$ is the equivalent linear stiffness matrix. The most commonly used method for determining $\boldsymbol{K}_{\mathrm{e}}$ is the force error minimization criterion, which requires the minimization of the difference between the nonlinear restoring force vector of the original system and the stiffness force vector of the equivalent system [12].

Defining Δ as

$$\Delta = \boldsymbol{\Gamma} - \boldsymbol{K}_{\mathrm{e}}\boldsymbol{X} \tag{3}$$

then

$$\mathrm{E}[\Delta^{\mathrm{T}}\Delta] \to \min \tag{4}$$

where E[ ] represents the mathematical expectation, and superscript T represents transpose. Eq. (4) implies that

$$\frac{\partial[\Delta^{\mathrm{T}}\Delta]}{\partial K_{\mathrm{e}ij}} = 0 \quad i,j = 1,2,\dots,N \tag{5}$$

Substituting Eq. (3) into Eq. (5) gives

$$\mathrm{E}[\boldsymbol{\Gamma}\boldsymbol{X}^{\mathrm{T}}] = \mathrm{E}[\boldsymbol{X}^{\mathrm{T}}\boldsymbol{X}]\boldsymbol{K}_{\mathrm{e}} \tag{6}$$

It is generally assumed that a weakly nonlinear system has a Gaussian response $\boldsymbol{X}$ when a Gaussian excitation $\boldsymbol{F}$ is applied. By using the following formula for the expected value of Gaussian vector $\boldsymbol{\eta}$ [12]

$$\mathrm{E}[f(\boldsymbol{\eta})\boldsymbol{\eta}^{\mathrm{T}}] = \mathrm{E}[\boldsymbol{\eta}^{\mathrm{T}}\boldsymbol{\eta}]\mathrm{E}\left[\frac{\partial f(\boldsymbol{\eta})}{\partial \boldsymbol{\eta}}\right] \tag{7}$$

Eq. (6) can be further expressed as

$$\mathrm{E}[\boldsymbol{X}^{\mathrm{T}}\boldsymbol{X}]\left[\mathrm{E}\left(\frac{\partial \boldsymbol{\Gamma}}{\partial \boldsymbol{X}}\right) - \boldsymbol{K}_{\mathrm{e}}\right] = \boldsymbol{0} \tag{8}$$

and the equivalent stiffness matrix of the nonlinear system can be written as

$$\boldsymbol{K}_{\mathrm{e}} = \mathrm{E}\left[\frac{\partial \boldsymbol{\Gamma}}{\partial \boldsymbol{X}}\right] \tag{9}$$

The expectation operator in Eq. (9) requires knowledge of the probability density function of the random response vector, which is unknown. Therefore, the equivalent linear solution procedure is programmed in an iterative fashion and some additional assumptions regarding the expectations of the response vector are required [12].

3 NLROM techniques and stiffness coefficients

There is a high computational cost to carry out EL analysis when considering structures with a large number of degrees of freedom. Muravyov and Rizzi [10] introduced NLROM techniques to drastically reduce the order of the models and effectively improve the computational efficiency of EL analysis. This approach also simplifies the expression of the nonlinear restoring force, which is beneficial to the formula derivation. In this section, referring to [10], NLROM techniques are introduced to reduce the computational cost of nonlinear random vibration problems. Also the process of the STEP method is optimized to determine nonlinear stiffness coefficients efficiently, according to the equivalence relationship.

3.1 Nonlinear reduced order modeling techniques

The following modal coordinate transformation is introduced into Eq. (1)

$$\boldsymbol{X} = \boldsymbol{\Phi q} \tag{10}$$

where $\boldsymbol{\Phi} = [\boldsymbol{\phi}_1, \boldsymbol{\phi}_2, \dots, \boldsymbol{\phi}_L]$ is the mass normalized modal matrix, L is the number of modal vectors and $\boldsymbol{q} = [q_1, q_2, \dots, q_L]^{\mathrm{T}}$ is the vector of modal coordinates. A set of coupled modal motion equations with reduced degrees of freedom is obtained as

$$\widetilde{\boldsymbol{M}}\ddot{\boldsymbol{q}} + \widetilde{\boldsymbol{C}}\dot{\boldsymbol{q}} + \widetilde{\boldsymbol{K}}\boldsymbol{q} + \boldsymbol{\gamma}(q_1, q_2, \dots, q_L) = \widetilde{\boldsymbol{F}} \tag{11}$$

where

$$\begin{aligned} \widetilde{\boldsymbol{M}} &= \boldsymbol{\Phi}^{\mathrm{T}}\boldsymbol{M}\boldsymbol{\Phi} = [\boldsymbol{I}] \\ \widetilde{\boldsymbol{C}} &= \boldsymbol{\Phi}^{\mathrm{T}}\boldsymbol{C}\boldsymbol{\Phi} = [2\zeta_r\omega_r] \\ \widetilde{\boldsymbol{K}} &= \boldsymbol{\Phi}^{\mathrm{T}}\boldsymbol{K}\boldsymbol{\Phi} = [\omega_r^2] \\ \boldsymbol{\gamma} &= \boldsymbol{\Phi}^{\mathrm{T}}\boldsymbol{\Gamma} \\ \widetilde{\boldsymbol{F}} &= \boldsymbol{\Phi}^{\mathrm{T}}\boldsymbol{F} \end{aligned} \tag{12}$$

$[\boldsymbol{I}]$ is the identity matrix. ζ_r and ω_r are the damping ratio and undamped natural frequency corresponding to the rth mode, respectively. $\boldsymbol{\gamma} = [\gamma_1, \gamma_2, \dots, \gamma_L]^{\mathrm{T}}$ is the nonlinear restoring force vector in modal space. According to Eq. (1) and Eq. (10), γ_r can be expressed as [10]

$$\gamma_r(q_1, q_2, \dots, q_L) = \sum_{j=1}^{L}\sum_{k=j}^{L} a_{jk}^r q_j q_k + \sum_{j=1}^{L}\sum_{k=j}^{L}\sum_{l=k}^{L} b_{jkl}^r q_j q_k q_l \quad (13)$$
$$r = 1,2, \dots, L$$

where a_{jk}^r and b_{jkl}^r are the nonlinear stiffness coefficients corresponding to the quadratic term $q_j q_k$ and the cubic term $q_j q_k q_l$ of the modal displacement, respectively, and the superscript r indicates the rth component γ_r of the modal nonlinear restoring force.

The considerable reduction in the number of degrees of freedom leads to a significant reduction in the computational cost of the response simulation. Determining the stiffness coefficients in Eq. (13) from a structural model is the core task of constructing a nonlinear reduced order model. Directly determining the nonlinear stiffness coefficients by the formula requires a specific finite element program and is not easily applied to complex engineering structures [24].Reference [18] proposed a STEP method to indirectly determine the nonlinear stiffness coefficients which does not require any internal information about the governing equations or the detailed formula for the system. This method enables the straightforward use of commercial codes such as NASTRAN and ABAQUS, and determines the nonlinear stiffness coefficients of complex engineering structures conveniently. However, the STEP method requires a series of static solutions to obtain the structural reaction forces, so there will be a massive cost if the number of modes is large.

3.2 STEP method and reduction in static solutions

The STEP method divides the nonlinear stiffness coefficients in Eq. (13) into three categories according to subscripts. By prescribing the displacement fields and obtaining the restoring forces using commercial codes, the equations satisfying these three categories of nonlinear stiffness coefficients are established, successively, to determine the respective nonlinear stiffness coefficients. First, the displacement fields are prescribed through the jth mode, so that only the stiffness coefficients with three identical subscripts (NCI) a_{jj}^r and b_{jjj}^r are retained in Eq. (13). Then, the displacement fields are prescribed by the jth and kth modes and equations satisfying the nonlinear stiffness coefficients with two different subscripts (NCD2) a_{jk}^r, b_{jjk}^r and b_{jkk}^r are established. Finally, the displacement field is prescribed by the jth, kth and lth modes, to establish a series of linear equations of the nonlinear stiffness coefficients with three different subscripts (NCD3) b_{jkl}^r. By prescribing forced displacement fields using modes and solving the three types of stiffness coefficients successively, the STEP method decomposes a large set of simultaneous equations in Eq. (13) into mutually independent equations determining all the stiffness coefficients with less effort. The detailed process of the STEP method is as follows.

1) Prescribing two displacement fields using the jth order mode as follows for $(1 \le j \le L)$

$$\boldsymbol{\phi}_j \bar{q}_j, \quad -\boldsymbol{\phi}_j \bar{q}_j \tag{14}$$

where $\bar{q}_j$ is a known non-zero scalar which is large enough to induce significant geometrically nonlinear effects but small enough to stay within the convergence limits of the finite element code [17]. Note that only the NCI related to the jth order mode appears in Eq. (13). The linear nodal restoring forces and the total nodal restoring forces of the structure under the forced displacement fields of Eq. (14) are obtained using a commercial finite element code, and then modal nonlinear restoring forces $\boldsymbol{\gamma}_j^{(1)}$ and $\boldsymbol{\gamma}_j^{(2)}$ are given by Eq.(1) and Eq. (12). Defining $\boldsymbol{A}_j$ as a matrix of NCI related to the jth order mode, Eq. (13) gives

$$\boldsymbol{A}_j = \boldsymbol{R}_j \boldsymbol{Q}_j \tag{15}$$

where

$$\boldsymbol{Q}_j = \frac{1}{2q_j^2}\begin{bmatrix} 1 & q_j^{-1} \\ 1 & -q_j^{-1} \end{bmatrix}, \qquad \boldsymbol{A}_j = \begin{bmatrix} a_{jj}^1 & b_{jjj}^1 \\ a_{jj}^2 & b_{jjj}^2 \\ \vdots & \vdots \\ a_{jj}^L & b_{jjj}^L \end{bmatrix}, \qquad \boldsymbol{R}_j = \begin{Bmatrix} \boldsymbol{\gamma}_j^{(1)} & \boldsymbol{\gamma}_j^{(2)} \end{Bmatrix} \tag{16}$$

2) Prescribing three displacement fields using the jth and kth order modes for $(1 \le j < k \le L)$

$$\boldsymbol{\phi}_j \bar{q}_j + \boldsymbol{\phi}_k \bar{q}_k, \quad -\boldsymbol{\phi}_j \bar{q}_j - \boldsymbol{\phi}_k \bar{q}_k, \quad \boldsymbol{\phi}_j \bar{q}_j - \boldsymbol{\phi}_k \bar{q}_k \tag{17}$$

let $\boldsymbol{\gamma}_{jk}^{(1)}$, $\boldsymbol{\gamma}_{jk}^{(2)}$ and $\boldsymbol{\gamma}_{jk}^{(3)}$ be the modal nonlinear restoring forces of the structure under those three forced displacement fields. Defining $\boldsymbol{B}_{jk}$ as a matrix of NCD2 related to the

jth and kth order modes, then

$$\boldsymbol{B}_{jk}=\left(\boldsymbol{P}_{jk}-\sum_{i=j,k}\boldsymbol{A}_i\boldsymbol{U}_i\right)\boldsymbol{S}_{jk} \tag{18}$$

where $\boldsymbol{A}_i$ has been obtained in Eq. (15),

$$\begin{gathered}\boldsymbol{P}_{jk}=\left\{\boldsymbol{\gamma}_{jk}^{(1)}\quad\boldsymbol{\gamma}_{jk}^{(2)}\quad\boldsymbol{\gamma}_{jk}^{(3)}\right\},\ \boldsymbol{U}_i=\bar{q}_i^2\begin{bmatrix}1 & 1 & 1\\ \bar{q}_i & -\bar{q}_i & \bar{q}_i\end{bmatrix}\\ \boldsymbol{S}_{jk}=\frac{1}{2q_jq_k}\begin{bmatrix}1 & 0 & q_k^{-1}\\ 1 & -q_j^{-1} & 0\\ 0 & -q_j^{-1} & q_k^{-1}\end{bmatrix},\ \boldsymbol{B}_{jk}=\begin{bmatrix}a_{jk}^1 & b_{jjk}^1 & b_{jkk}^1\\ a_{jk}^2 & b_{jjk}^2 & b_{jkk}^2\\ \vdots & \vdots & \vdots\\ a_{jk}^L & b_{jjk}^L & b_{jkk}^L\end{bmatrix}\end{gathered} \tag{19}$$

3) Prescribing a displacement field as follows using the jth, kth and lth order modes for $(1\le j<k<l\le L)$

$$\boldsymbol{\phi}_j\bar{q}_j+\boldsymbol{\phi}_k\bar{q}_k+\boldsymbol{\phi}_l\bar{q}_l \tag{20}$$

is the modal nonlinear restoring force of the structure under the forced displacement field. Defining $\boldsymbol{C}_{jkl}$ as a matrix of NCD3 related to the jth, kth and lth order modes, then

$$\boldsymbol{C}_{jkl}=\frac{1}{q_jq_kq_l}\left(\boldsymbol{\gamma}_{jkl}-\sum_{i=j,k,l}\boldsymbol{A}_i\boldsymbol{V}_i-\sum_{in=jk,jl,kl}\boldsymbol{B}_{in}\boldsymbol{W}_{in}\right) \tag{21}$$

where $\boldsymbol{A}_i$ and $\boldsymbol{B}_{in}$ have been obtained in Eq. (15) and Eq. (18), respectively,

$$\boldsymbol{C}_{jkl}=\begin{bmatrix}b_{jkl}^1\\ b_{jkl}^2\\ \vdots\\ b_{jkl}^L\end{bmatrix},\qquad \boldsymbol{V}_i=\bar{q}_i^2\begin{Bmatrix}1\\ \bar{q}_i\end{Bmatrix},\ \boldsymbol{W}_{in}=\bar{q}_i\bar{q}_n\begin{Bmatrix}1\\ \bar{q}_i\\ \bar{q}_n\end{Bmatrix} \tag{22}$$

All nonlinear stiffness coefficients in the reduced order models are classified and successively determined by the above three steps.

The STEP method directly determines all the nonlinear stiffness coefficients in the reduced order models with little effort. It is worthwhile to note that the nonlinear elastic potential is related to the nonlinear elastic forces via the expression [10]

$$\gamma_r = \frac{\partial U}{\partial q_r}, \qquad r = 1,2,\dots,L \tag{23}$$

Substituting Eq. (13) gives

$$\frac{\partial \gamma_j}{\partial q_k} = \frac{\partial \gamma_k}{\partial q_j} = \frac{\partial^2 U}{\partial q_j q_k} \tag{24}$$

The symmetry relations were used to assess how well the identification had been performed, but in practice, the STEP method rarely gives wrong stiffness coefficients results. At the same time, when the number of reduced modes is large, it is cumbersome to determine the matching of specific two coefficients in a large number of stiffness coefficients. Therefore, in this paper, the symmetry relations in Eq. (24) are taken as constraints to reduce the calculation cost.

The ranges of the subscript of the NCD2 and NCD3 are divided into several intervals, and a set of partial intervals is given. If the stiffness coefficients in the given intervals are determined directly by Eqs. (14)-(22), all the stiffness coefficients in the remaining

intervals can be determined indirectly by the equivalence relationship of Eq. (24). Then, an improved process for determining the stiffness coefficients is developed based on the STEP method, which automatically identifies the optimized interval for any number of modes, directly determines the stiffness coefficients in the given intervals and indirectly determines the remainders. The improved method avoids part of the static solutions by taking advantage of the properties of Eq. (24), and a notable reduction in the computational cost in determining the nonlinear stiffness coefficients is achieved. The improved process includes six steps as follows.

1) Determining all of NCI using Eq. (14) and Eq. (15).

2) The value range of NCD2 subscripts is divided into three intervals by $L/2$, $1 \le j < k \le L/2$, $L/2 \le j < k \le L$ and $1 \le j < L/2 \le k \le L$. On the one hand, it keeps the symmetry of the intervals and facilitates the implementation of equivalence relations in Eq. (24). On the other hand, fewer intervals simplify the calculation process. The displacement fields in Eq. (17) are prescribed using the jth and kth modes for ($1 \le j < k \le L/2$ or $L/2 \le j < k \le L$), and NCD2 in the first and second intervals are determined using Eq. (18).

3) a_{jk}^{r} for $(1 \le r < L)$, b_{jjk}^{r} for $(1 \le r < L/2)$ and b_{jkk}^{r} for $(L/2 \le r \le L)$ in the third interval are determined indirectly by NCI in step 1) and NCD2 in step 2) using the equivalence relations.

4) Prescribing the first displacement fields in Eq. (17) using the jth and kth

modes for $(1 \le j < k \le L/2$ or $L/2 \le j < k \le L)$, then b_{jjk}^{r} for $1 \le r < L/2$ and b_{jkk}^{r} for $L/2 \le r \le L$ in the third interval are determined. It is worth noting that all of the NCD2 are determined in steps 2) to 4).

5) The range of values of NCD3 subscripts is divided into four intervals, $1 \le j < k < l \le L/2, 1 \le j < k \le L/2 < l \le L, 1 \le j \le L/2 < k < l \le L$ and $L/2 \le j < k < l \le L$. Prescribing the displacement field in the Eq. (20) using the jth, kth and lth modes for $(1 \le j < k < l \le L/2$ or $1 \le j < k \le L/2 < l \le L$ or $L/2 \le j < k < l \le L)$, the NCD3 in the first, second and fourth intervals are determined using Eq. (21).

6) The NCD3 in the third interval is determined indirectly by the NCD2 in steps 2) to 4) and NCD3 in step 5). All nonlinear stiffness coefficients are determined directly or indirectly by the above six steps.

Fig. 2 and Fig. 3 show comparisons for the static solutions of the STEP method and the improved STEP method in determining the stiffness coefficients. The orange parts of the figures represent that three static solutions under prescribed displacement fields are required for each cycle, while the blue parts require only one.

The derivation of Eq. (24) is accurate, thus there is little inaccuracy in determining stiffness coefficients. The total number of static solutions of the STEP method is

$$N_{\mathrm{s}} = \frac{L^3 + 6L^2 + 5L}{3} \tag{25}$$

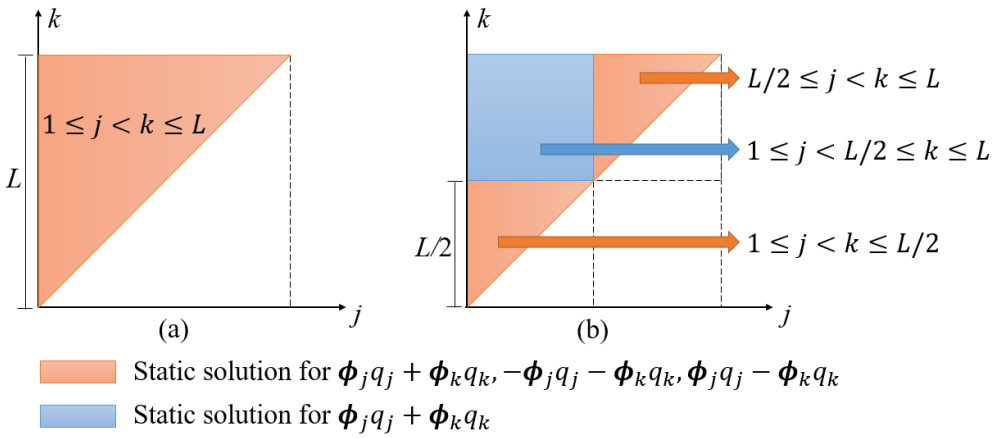

Fig. 2 Comparison of the static solutions in determining NCD2

(a) STEP method; (b) Improved STEP method

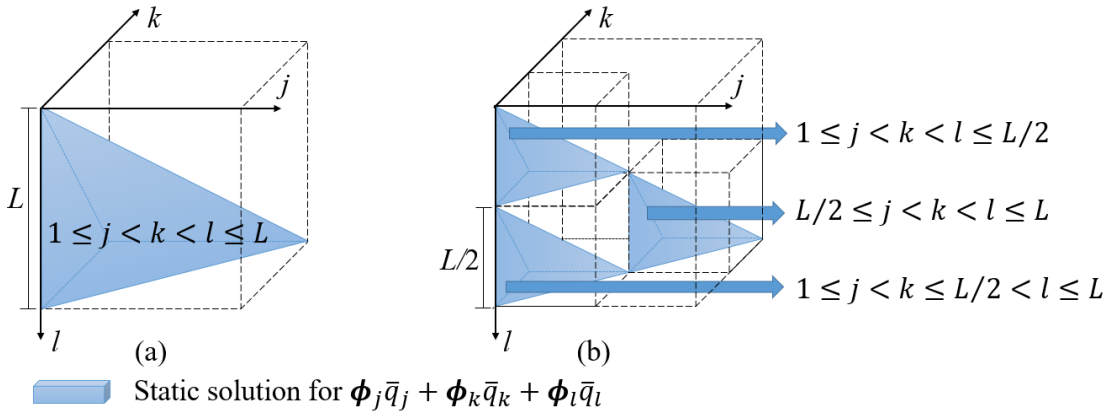

Fig. 3 Comparison of the static solutions in determining NCD3

(a) STEP method; (b) Improved STEP method

while that of the improved STEP method proposed in this paper is

$$\begin{aligned} N_{\mathrm{s}} &= \frac{5L^3 + 30L^2 + 40L}{24}, \quad L \text{ even} \\ N_{\mathrm{s}} &= \frac{5L^3 + 27L^2 + 27L + 21}{24}, \quad L \text{ odd} \end{aligned} \tag{26}$$

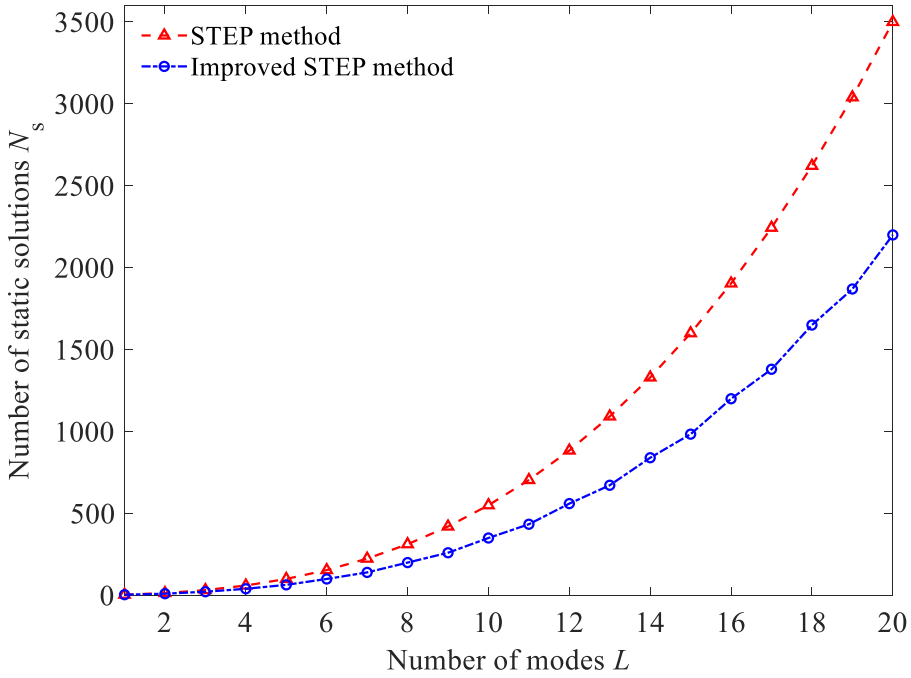

Fig. 4 Comparison for total number of static solutions

Fig. 4 shows the comparison of the total number of static calculations required for the STEP method and the improved STEP method. In cases where a considerable number of modes are employed, such as the reduced order models in [25], [26], the improved STEP method achieves a notable computational saving and never requires a deep insight into calculation core of commercial finite element software.

4 EL method modified by higher order statistics

The NLROM-EL method replaces the nonlinear terms by the linear terms directly. As a result, the linearized system does not contain statistical information higher than the second-order, which yields some error. The REL method was proposed to improve the accuracy of the EL method and has been applied for the vibration problems of the Duffing oscillator [13] and a beam model [15], [16]. The reduced order models introduced in Section 3 include nonlinear terms $q_j q_k^2$, $q_j^2 q_k$ and $q_j q_k q_l$, so the REL method leads to

different equivalent results, increasing the complexity of the solution. To solve this problem, this paper proposes a new scheme based on references [15],[16] to unify the equivalent results of nonlinear terms. Besides, the new scheme has a concise and regular form giving the equivalent result of Eq. (14) with less effort.

4.1 Modal motion equation with higher order statistics

The difference of the powers of $q_j q_k^2$ and $q_j^2 q_k$ are 2 and 1 when replaced by the linear term q_j, while those are the opposite when replaced by q_k. Therefore the same nonlinear terms are equivalent to different higher order terms according to the chosen scheme of the REL method. To resolve the difference, a new regulated scheme is proposed, in which the nonlinear terms in Eq. (13) are equivalent to

$$\begin{aligned}\hat{\gamma}_r(q_1, q_2, \cdots, q_L) &= \sum_{j=1}^{L}\sum_{k=j}^{L} a_{jk}^r q_j q_k + \sum_{j=1}^{L} \hat{b}_{jjj}^r q_j^5 + \sum_{j=1}^{L-1}\sum_{k=j+1}^{L} \hat{b}_{jjk}^r q_j^4 q_k \\ &+ \sum_{j=1}^{L-1}\sum_{k=j+1}^{L} \hat{b}_{jkk}^r q_j q_k^4 + \sum_{j=1}^{L-2}\sum_{k=j+1}^{L-1}\sum_{l=k+1}^{L} b_{jkl}^r q_j q_k q_l\end{aligned} \tag{27}$$

The scheme requires that the minimization of the difference between Eq. (13) and Eq. (27). If $\mathrm{D}[z]$ represents the mean square value of z,

$$\begin{gathered}\mathrm{D}\left[\hat{b}_{jjj}^r q_j^5 - b_{jjj}^r q_j^3\right] \to \min \\ \mathrm{D}\left[\hat{b}_{jjk}^r q_j^4 q_k - b_{jjk}^r q_j^2 q_k\right] \to \min,\ \ \mathrm{D}\left[\hat{b}_{jkk}^r q_j q_k^4 - b_{jkk}^r q_j q_k^2\right] \to \min\end{gathered} \tag{28}$$

Defining

$$\mathcal{F}[z_0, z_1, z_2, \dots, z_n] = \frac{(\mathrm{E}[z_0])^n}{\mathrm{E}[z_1]\mathrm{E}[z_2]\cdots\mathrm{E}[z_n]} \tag{29}$$

then Eq. (28) gives

$$\begin{gathered} \hat{b}^r_{jjj} = b^r_{jjj}\mathcal{F}\left[q_j^8, q_j^{10}\right] \\ \hat{b}^r_{jjk} = b^r_{jjk}\mathcal{F}\left[q_j^6 q_k^2, q_j^8 q_k^2\right], \quad \hat{b}^r_{jkk} = b^r_{jkk}\mathcal{F}\left[q_j^2 q_k^6, q_j^2 q_k^8\right] \end{gathered} \tag{30}$$

and $\hat{\gamma}_r$ are replaced by cubic nonlinear terms

$$\bar{\gamma}_r(q_1, q_2, \dots, q_L) = \sum_{j=1}^{L}\sum_{k=j}^{L} a^r_{jk} q_j q_k + \sum_{j=1}^{L}\sum_{k=j}^{L}\sum_{l=k}^{L} \bar{b}^r_{jkl} q_j q_k q_l \tag{31}$$

By performing operations similar to Eq. (28) and Eq. (30), a regulated form of the nonlinear stiffness coefficients is obtained,

$$\begin{gathered} \bar{b}^r_{jkl} = b^r_{jkl}, \quad \text{for } 1 \le j < k < l \le L \\ \bar{b}^r_{jkl} = b^r_{jkl}\mathcal{F}\left[q_j^8, q_j^{10}, q_j^6\right], \quad \text{for } 1 \le j = k = l \le L \\ \bar{b}^r_{jkl} = b^r_{jkl}\mathcal{F}\left[q_j^6 q_k^2, q_j^8 q_k^2, q_j^4 q_k^2\right], \quad \text{for } 1 \le j = k < l \le L \\ \bar{b}^r_{jkl} = b^r_{jkl}\mathcal{F}\left[q_j^2 q_k^6, q_j^2 q_k^8, q_j^2 q_k^4\right], \quad \text{for } 1 \le j < k = l \le L \end{gathered} \tag{32}$$

For a series of zero-mean Gaussian random processes $z_i (i = 1,2, \dots)$, the following relationship holds [15]

$$\mathrm{E}[z_1 z_2 \ldots z_{2m}] = \sum_{\text{all independent pairs}} \left[\prod_{j \neq k} \mathrm{E}[z_j z_k] \right] \tag{33}$$

where m is a positive integer, the number of independent pairs is $2m!/(2^m m!)$ and

$$\mathrm{E}[z_1 z_2 \ldots z_{2m-1}] = 0 \tag{34}$$

For the weakly nonlinear system to which the classical EL method is applied, the response $\boldsymbol{q}$ is considered to obey the zero-mean Gaussian distribution. Therefore, higher order statistics in Eq. (32) can be expressed by the second-order statistics of response, and reduced order equations of motion with improved nonlinear terms are obtained as

$$\widetilde{\boldsymbol{M}}\ddot{\boldsymbol{q}} + \widetilde{\boldsymbol{C}}\dot{\boldsymbol{q}} + \widetilde{\boldsymbol{K}}\boldsymbol{q} + \overline{\boldsymbol{\gamma}}(q_1, q_2, \ldots, q_L) = \widetilde{\boldsymbol{F}} \tag{35}$$

4.2 Equivalent linearization analysis

The reduced order equation of motion in Eq. (35) can also be equivalenced to a linearized system, according to the derivation in Section 2

$$\widetilde{\boldsymbol{M}}\ddot{\boldsymbol{q}} + \widetilde{\boldsymbol{C}}\dot{\boldsymbol{q}} + \left(\widetilde{\boldsymbol{K}} + \widetilde{\boldsymbol{K}}_{\mathrm{e}}\right)\boldsymbol{q} = \widetilde{\boldsymbol{F}} \tag{36}$$

where $\widetilde{\boldsymbol{K}}_{\mathrm{e}}$ is the fully populated modal equivalent linear stiffness matrix. Applying Eqs. (3)-(9) gives

$$\widetilde{\boldsymbol{K}}_{\mathrm{e}} = \mathrm{E}\left[\frac{\partial \overline{\boldsymbol{\gamma}}}{\partial \boldsymbol{q}}\right] \tag{37}$$

Define $\mathcal{A}(m,n) = \sum_{j=1}^{L} a_{jn}^{m} \mathrm{E}[q_j]$ and $\mathcal{B}(m,n) = \sum_{j=1}^{L} \sum_{k=j}^{L} \bar{b}_{jkn}^{m} \mathrm{E}[q_j q_k]$. Substituting Eq. (35) into the Eq. (36) gives

$$\widetilde{\boldsymbol{K}}_{\mathrm{e}} = \begin{bmatrix} \mathcal{A}(1,1) + \mathcal{B}(1,1) & \cdots & \mathcal{A}(1,L) + \mathcal{B}(1,L) \\ \vdots & \ddots & \vdots \\ \mathcal{A}(L,1) + \mathcal{B}(L,1) & \cdots & \mathcal{A}(L,L) + \mathcal{B}(L,L) \end{bmatrix} \tag{38}$$

Since a zero-mean response is assumed, $\mathcal{A}(m,n) = 0$ for any m, n, so that

$$\widetilde{\boldsymbol{K}}_{\mathrm{e}} = \begin{bmatrix} \mathcal{B}(1,1) & \cdots & \mathcal{B}(1,L) \\ \vdots & \ddots & \vdots \\ \mathcal{B}(L,1) & \cdots & \mathcal{B}(L,L) \end{bmatrix} \tag{39}$$

The equivalent linear stiffness matrix is a function of the unknown modal displacement response. The solution to Eq. (36) takes an iterative form, i.e.,

$$\widetilde{\boldsymbol{M}}\ddot{\boldsymbol{q}}^{m} + \widetilde{\boldsymbol{C}}\dot{\boldsymbol{q}}^{m} + \left(\widetilde{\boldsymbol{K}} + \widetilde{\boldsymbol{K}}_{\mathrm{e}}^{m-1}\right)\boldsymbol{q}^{m} = \widetilde{\boldsymbol{F}} \tag{40}$$

where superscript m is the iteration number. At the start of the first iteration $\widetilde{\boldsymbol{K}}_{\mathrm{e}}^{0} = \boldsymbol{0}$. Assuming a stationary system and excitation, the random response of Eq. (40) is

$$\tilde{\boldsymbol{S}}_{qq}^{m}(\omega) = \widetilde{\boldsymbol{H}}^{m-1}(\omega)\tilde{\boldsymbol{S}}_{ff}(\omega)\left[\widetilde{\boldsymbol{H}}^{m-1}(\omega)\right]^{\mathrm{T}} \tag{41}$$

where $\tilde{\boldsymbol{S}}_{qq}$ and $\tilde{\boldsymbol{S}}_{ff}$ are the power spectral density (PSD) of the modal displacement and excitation, respectively. $\widetilde{\boldsymbol{H}}$ is the frequency response matrix given by

$$\widetilde{\boldsymbol{H}}^{m-1}(\omega) = \left(-\omega^2\widetilde{\boldsymbol{M}} + \mathrm{i}\omega\widetilde{\boldsymbol{C}} + \widetilde{\boldsymbol{K}} + \left[\alpha\widetilde{\boldsymbol{K}}_{\mathrm{e}}^{m-1} + \beta\widetilde{\boldsymbol{K}}_{\mathrm{e}}^{m-2}\right]\right) \tag{42}$$

where α and β are weightings to aid the convergence of the solution with $\alpha+\beta=1$, generally $\alpha=\beta=0.5$. Note that, in modal coordinates, the order of the matrices in Eq. (42) is not large, so it is not difficult to calculate the frequency response matrix. The covariance matrix of the modal displacement response is given by the Wiener-Khinchin formula as

$$\mathrm{E}[q_r q_s]^m = R^m_{q_r q_s}(0) = \int_{\omega_\mathrm{l}}^{\omega_\mathrm{u}} \tilde{S}^m_{q_r q_s}(\omega)\mathrm{d}\omega \tag{43}$$

where ω_l and ω_u are the lower and upper limits of the excitation frequency band. Especially, when subjected to white noise, the covariance moment can be obtained from the Lyapunov equations instead of integration. The iterations continue until convergence of the modal equivalent linear stiffness matrix is achieved, such that

$$\frac{\sum_{j=1}^{L}\sum_{k=j}^{L}\left|\widetilde{\boldsymbol{K}}^m_{\mathrm{e}jk}-\widetilde{\boldsymbol{K}}^{m-1}_{\mathrm{e}jk}\right|}{L^2\left|\widetilde{\boldsymbol{K}}^m_{\mathrm{e}}\right|_{\max}}<\varepsilon \tag{44}$$

where $\left|\widetilde{\boldsymbol{K}}^m_{\mathrm{e}}\right|_{\max}$ is the entry of $\widetilde{\boldsymbol{K}}_{\mathrm{e}}$ with the largest absolute value, and typically $\varepsilon=0.001$. Following convergence of $\widetilde{\boldsymbol{K}}_{\mathrm{e}}$, the covariance matrix of the displacement in physical coordinates is recovered from

$$\mathrm{E}\left[x_i x_j\right] = \boldsymbol{\Phi}\mathrm{E}[q_r q_s]\boldsymbol{\Phi}^T \tag{45}$$

Only a few basic operations are added to the proposed method to calculate the regulated

form of the stiffness coefficients, and therefore there is little increase in the computational cost compared with the NLROM-EL method. At the same time, it is worthwhile to note that the zero mean Gaussian assumption introduced in Eq. (33) is also used in the traditional EL method, that is, Eq. (6) and Eq. (7). Therefore, the proposed method is also applicable to the solution of random vibration problems of weakly nonlinear systems.

5 Numerical examples

First, the efficiency and accuracy of the improved STEP method and the EL method improved by the higher order statistics proposed in this paper are verified using examples from reference [10]. Then the random response of composite laminated plates under band-limited white noise or a turbulent boundary layer is predicted using the NLROM-EL method, time-domain numerical simulation and the EL method proposed in this paper. A flowchart for the solution procedure of the proposed method is shown in Fig. 5.

5.1 Verification of methods

Consider the simply supported rectangular aluminum plate model shown in Fig. 1. The plate measures 0.3556m in length, 0.254m in width, 0.00102m in thickness, and the Young's modulus, Poisson's ratio and mass density are 7.3×10^{10}Pa, 0.3 and 2763kg/m^3, respectively. A NASTRAN model of the full plate was built with a uniform 56×40 mesh of 2240 CQUAD4 elements.

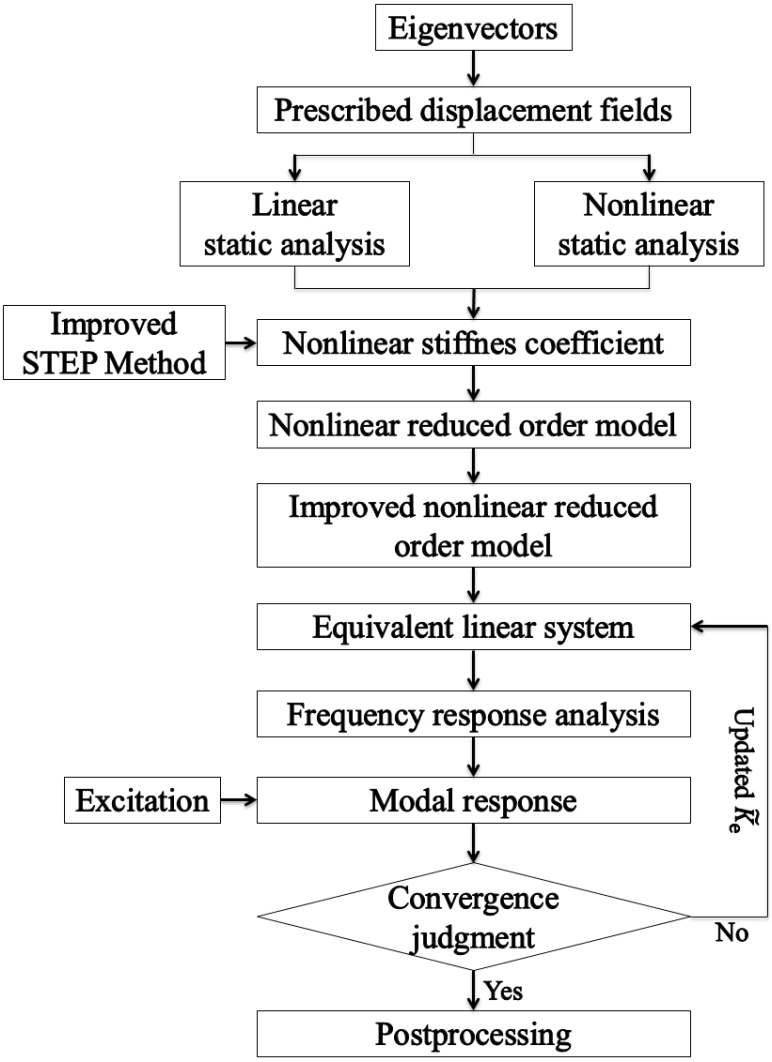

Fig. 5 Flowchart for the solution procedure of the proposed method

Although the derivation of Eq.(24) is analytical, a large number of nonlinear static problems need to be solved in the actual operation process. Thus the error caused by iterative calculations means that the stiffness coefficients determined by the improved STEP method and the STEP method will not be exactly the same. Therefore, it is necessary to evaluate the improved STEP method to verify the quality and efficiency of

establishing NLROM. Considering the example of a metal plate under uniformly distributed pressure in reference [10], the reduced order model of the plate was constructed using the first eight symmetrical modes. The total number of static solutions required to determine the stiffness coefficients was 312 by the STEP method and 200 by the improved STEP, a reduction of 36%. The deflection of the midpoint of the plate was calculated by NASTRAN SOL106 and the STEP method, and the results are shown in Fig. 6. It can be observed that the results of NLROM constructed by the two methods are very similar, indicating that the stiffness coefficients determined by the improved STEP method can be used to replace those determined by the STEP method while ensuring the quality of the constructed NLROM and achieving high computational efficiency.

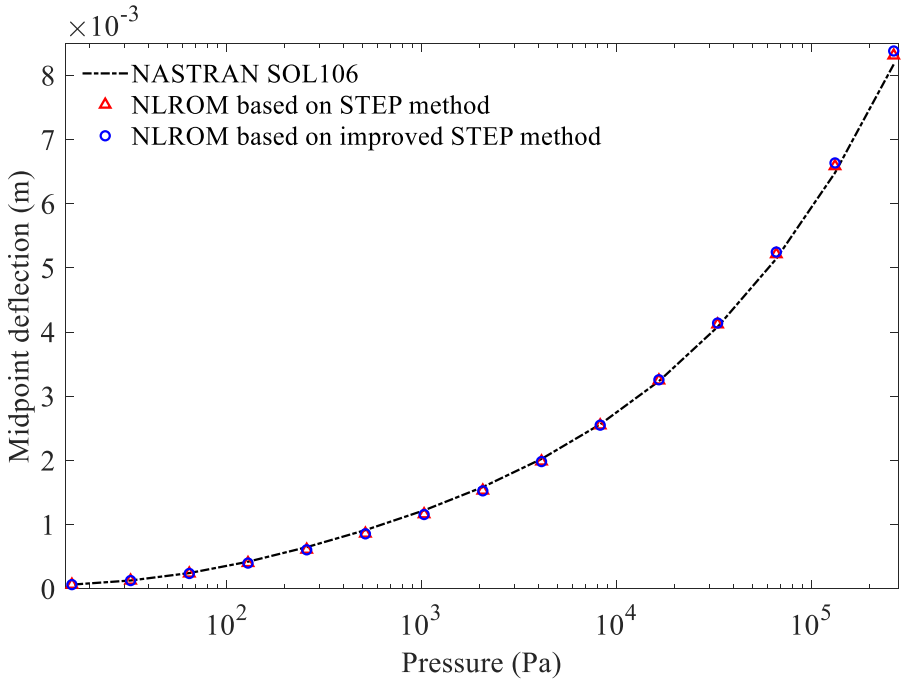

Fig. 6 Deflection at midpoint of the plate

Next, an example of a metal plate subjected to band-limited white noise is considered. The frequency band of the excitation is $\omega_{\mathrm{l}} = 0\mathrm{Hz}$ to $\omega_{\mathrm{u}} = 1024\mathrm{Hz}$ and the sound pressure level (SPL) ranges from 106dB to 160dB, in 6dB increments. The one-sided PSD function of Gaussian band-limited white noise is given as follows [19]

$$S_{ff}(\omega) = \begin{cases} \dfrac{p_0^2}{\Delta\omega} 10^{\mathrm{SPL}/10}, & \omega_{\mathrm{l}} \le \omega \le \omega_{\mathrm{u}} \\ 0, & \text{otherwise} \end{cases} \tag{46}$$

where $p_0 = 2 \times 10^{-5}\mathrm{Pa}$ is the reference pressure, ω is the frequency and $\Delta\omega = \omega_{\mathrm{u}} - \omega_{\mathrm{l}}$ is the bandwidth of the excitation.

As in [10], the first two symmetrical modes of the structure are selected to participate in the EL analysis. The corresponding damping ratios are 2% and 0.54%, respectively. The NLROM-EL method, time-domain numerical simulation and the proposed method are used to predict the root mean square (RMS) value of the midpoint displacement response of the plate, where the time-domain numerical simulation results are directly taken from [10], and the RMS results are shown in Fig. 7. Furthermore, the error of the NLROM-EL method and the proposed method with respect to the time-domain numerical simulation is given in Fig. 8. It can be observed that the accuracy of the proposed method is better than that of the NLROM-EL method in most cases. However, it is slightly worse in the case of 124dB, but the error is still less than 5% and is entirely acceptable. Comparisons of the computational time and iteration counts are given in Fig. 9.

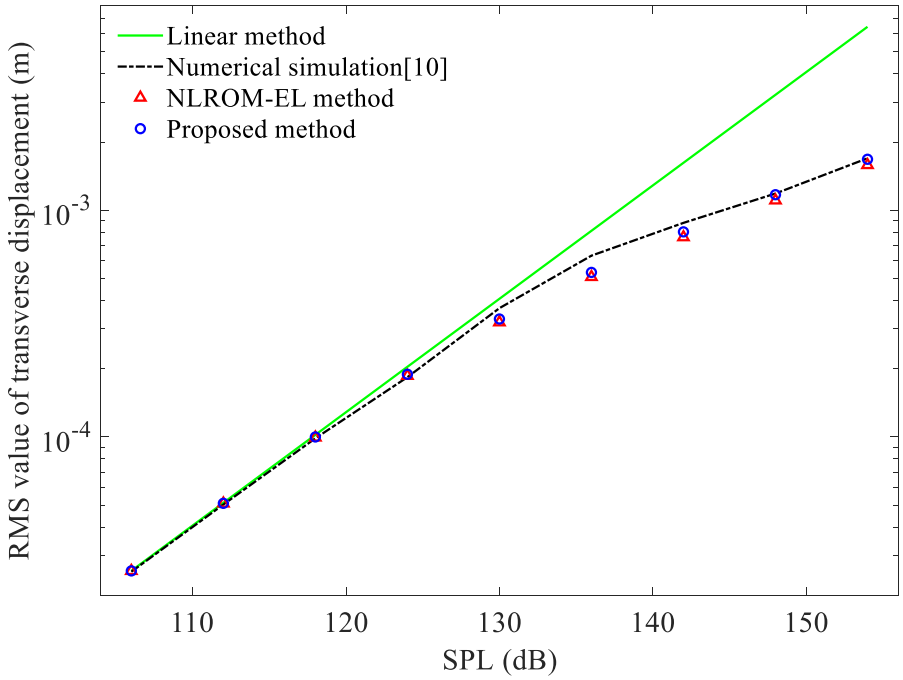

Fig. 7 Comparison of RMS value of midpoint displacement response

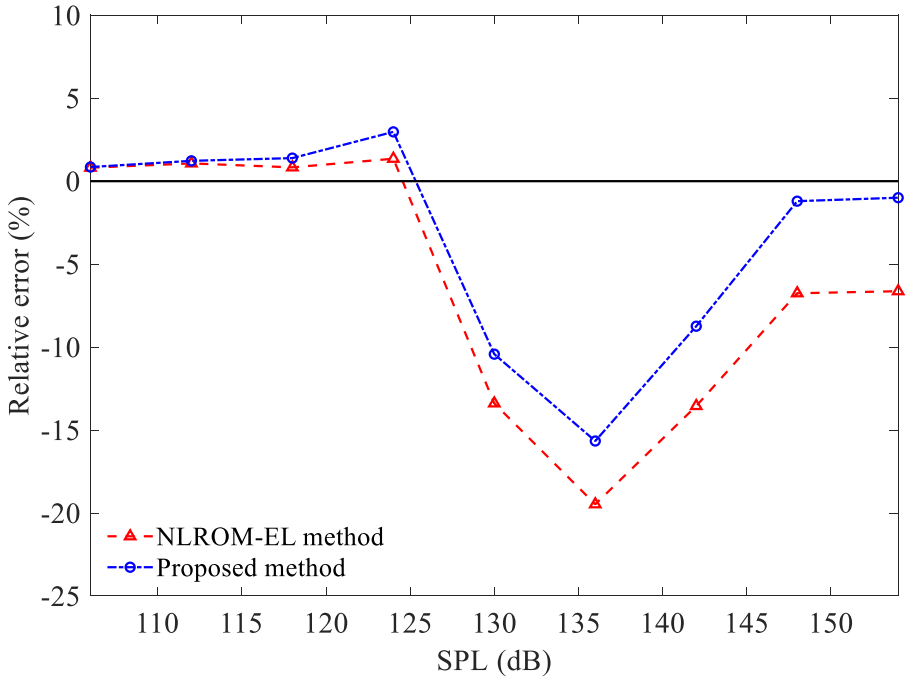

Fig. 8 Comparison of computational error

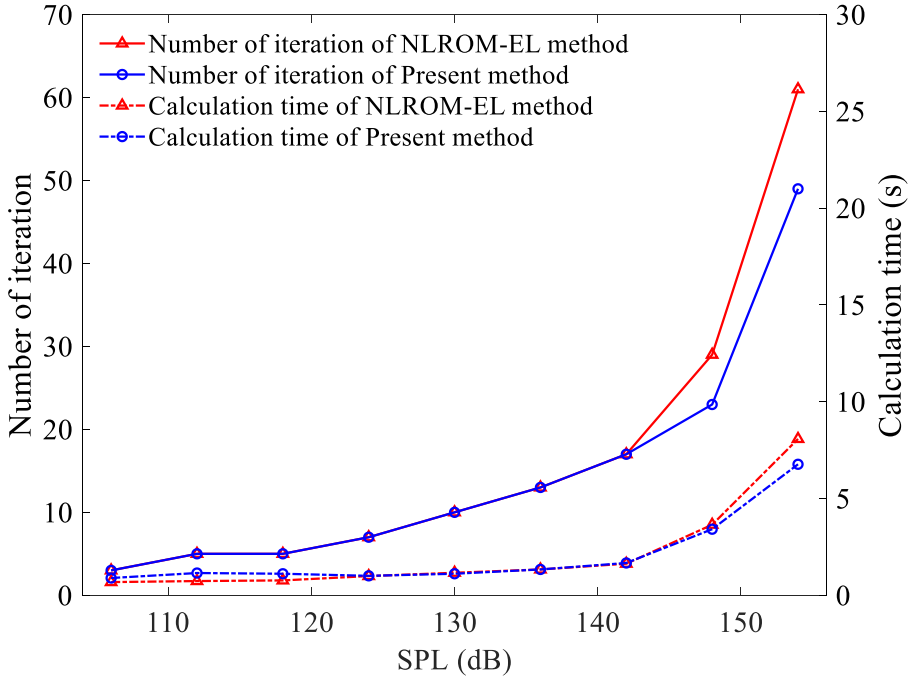

Fig. 9 Comparisons of computational time and iteration counts

5.2 Random response of laminated plates

Two rectangular, simply supported eight-layered laminated plates taken from [19] were investigated, including symmetric [0°/90°/0°/90°/90°/0°/90°/0°] and antisymmetric [0°/90°/0°/90°/0°/90°/0°/90°] cross-ply laminated plates. The laminated plates keep the same geometric dimension and mesh size as the metal plate in Section 5.1, and have mass density 1600kg/m^3, Young's moduli E_{11}=1.81×10^{11}Pa, E_{22}=1.03×10^{10}Pa, shear moduli G_{12}=G_{13}=7.17×10^{9}Pa, G_{23}=5×10^{9}Pa and Poisson's ratio 0.28. The first five modes were selected for EL analysis. The damping ratio of the first mode is $\zeta_1 = 0.02$ and those of the first five modes meet the requirement that $2\omega_1\zeta_1 = 2\omega_2\zeta_2 = \cdots = 2\omega_5\zeta_5$. The result in reference [19] also shows that the response of an antisymmetric cross-ply laminated

plate subjected to band-limited white noise can still be approximately considered to obey the zero mean Gaussian distribution.

First, consider the load case investigated in [19] where the laminated plates were subjected to band-limited white noise, whose bandwidth and SPL are the same as the excitation used in Section 5.1. Since [19] does not give the reference solutions, in this paper, the RMS value of the random response of laminated plates under the band-limited white noise is obtained in a series of time-domain numerical simulation, which were carried out by ABAQUS referring to [5] -[7]. The laminated plates were modeled with a uniform 28×20 mesh of 560 S4R elements, twice the size as those of the NASTRAN model, to reduce the computational time referring to [10]. The time series of the band-limited white noise is simulated by [27]

$$f(t_m) = \sqrt{2}\sum_{n=0}^{N-1}\left[S_{ff}\Delta\omega\right]^{\frac{1}{2}}\cos(\omega_n t_m - \phi_n) \tag{47}$$

where S_{ff} is the one-sided PSD function, f is the simulated series of the excitation, $t_m = m\Delta t$ is the discrete time series, Δt is the length of the time step, M is the number of discrete time steps, ϕ_n is a uniformly distributed random number on the interval $(0 - 2\pi)$, $\omega_n = n\Delta\omega$ is the discrete frequency series, $\Delta\omega = (\omega_{\mathrm{u}} - \omega_{\mathrm{l}})/N$ is the length of the frequency step, N is the number of discrete frequency steps. M and N should be large integers. A total of 10 independent time-domain simulations were carried out, with $M = 2^{16}$, $\Delta t = 5 \times 10^{-5}\mathrm{s}$, $\Delta\omega = 2\pi$.

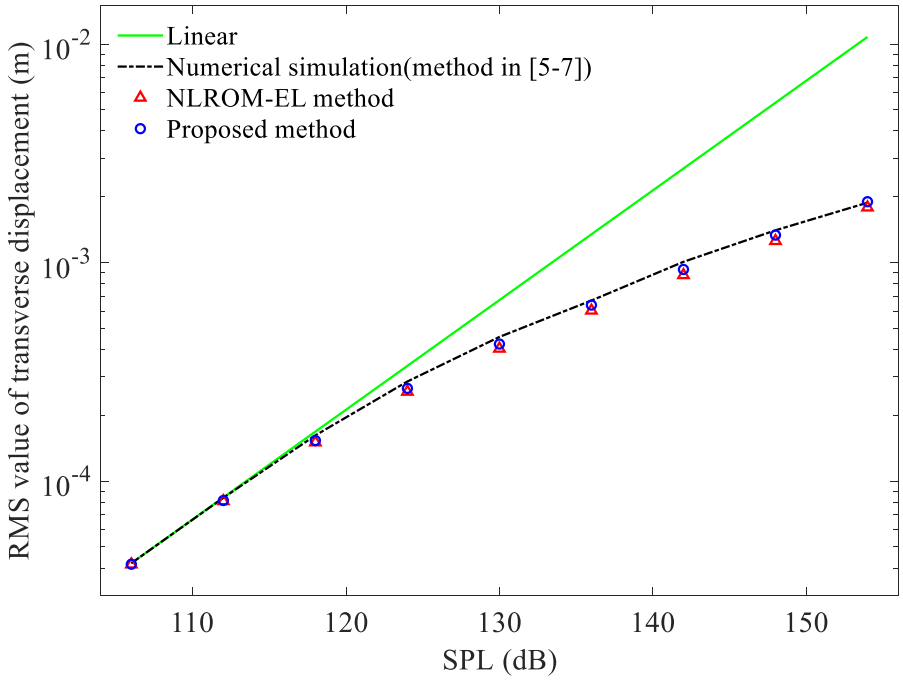

(a) Symmetric cross-ply laminated plate

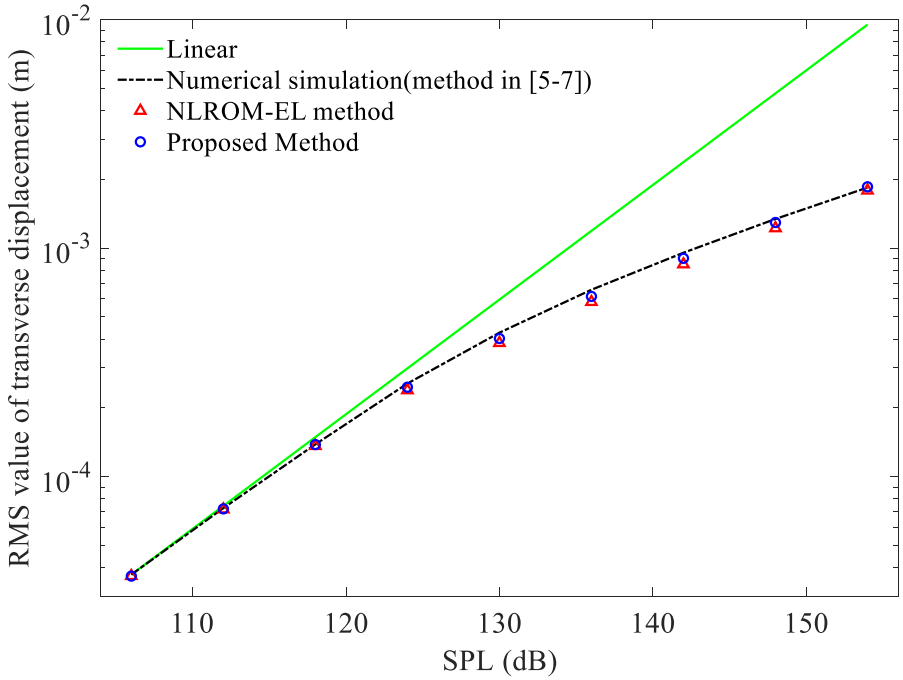

(b) Antisymmetric cross-ply laminated plate

Fig. 10 Comparison of RMS value of midpoint displacement response

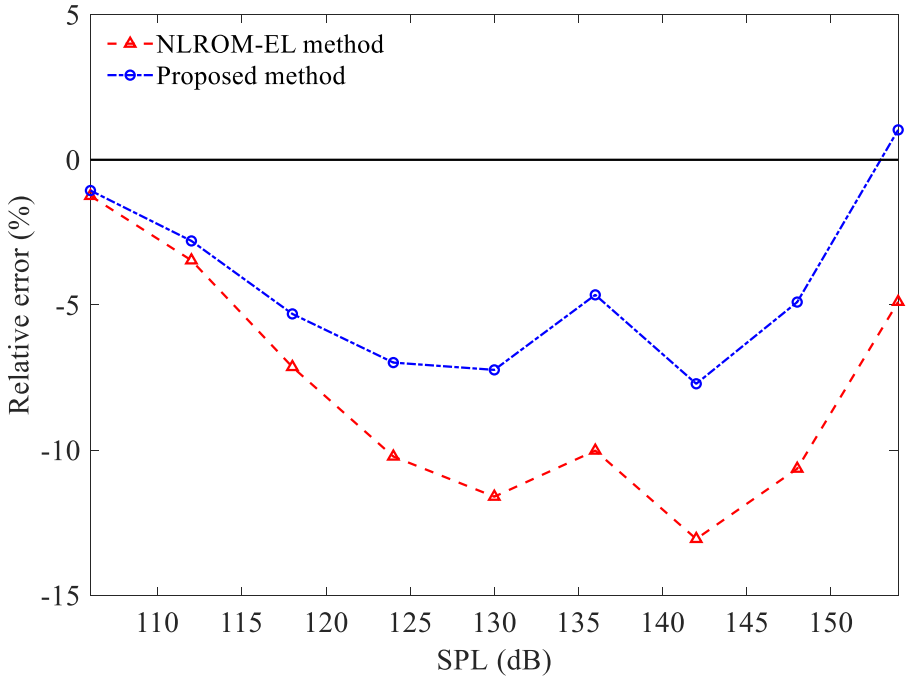

(a) Symmetric cross-ply laminated plate

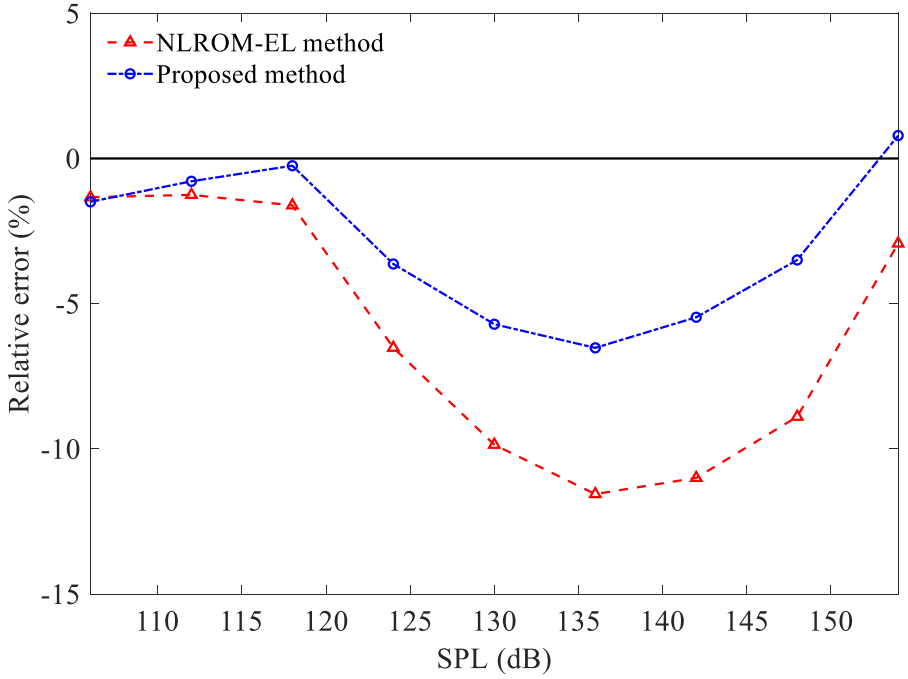

(b) Antisymmetric cross-ply laminated plate

Fig. 11 Comparison of computational error

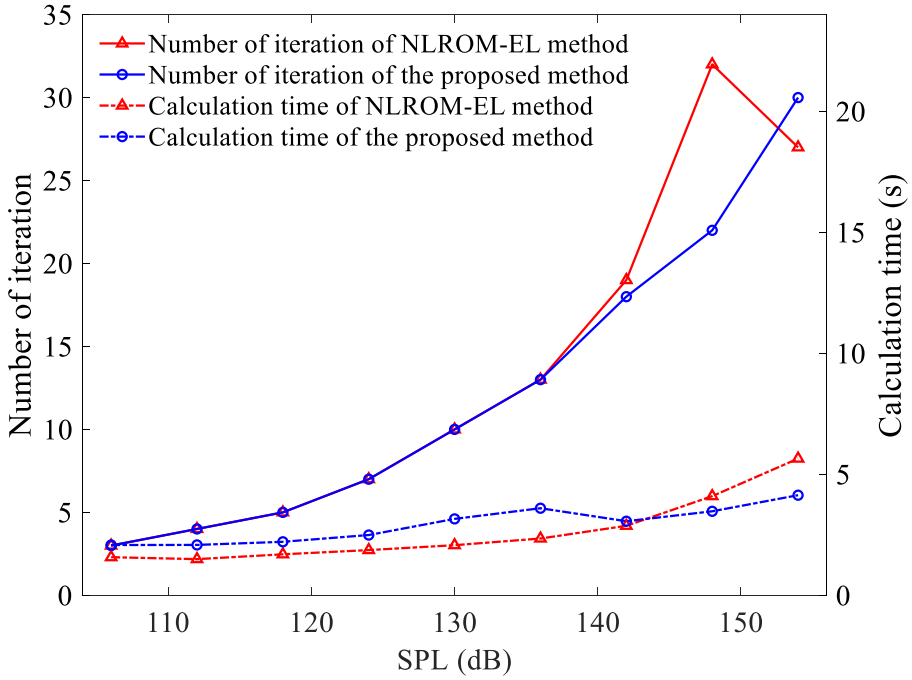

(a) Symmetric cross-ply laminated plate

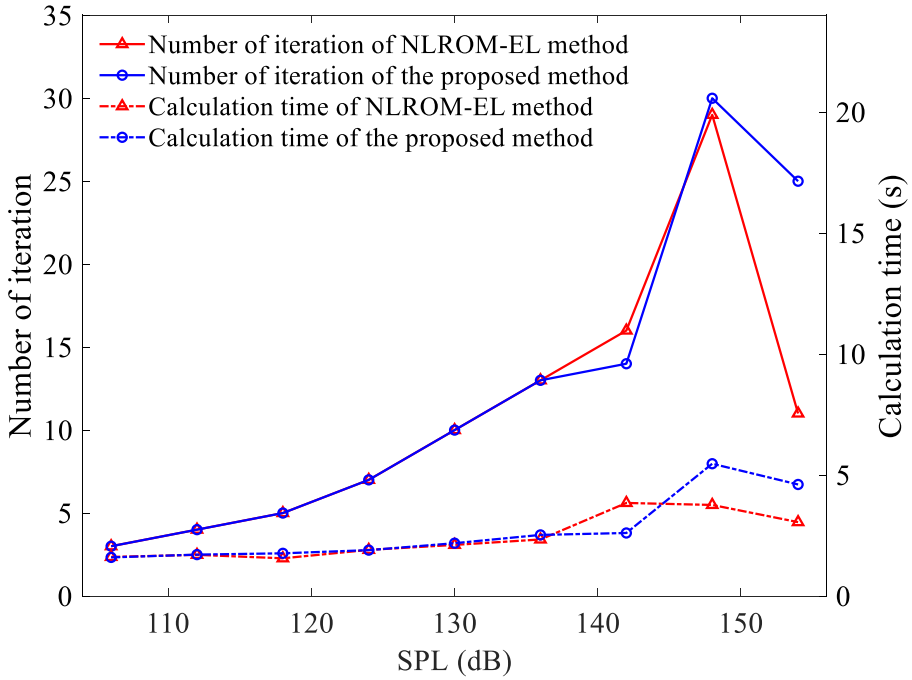

(b) Antisymmetric cross-ply laminated plate

Fig. 12 Comparisons of computational time and iteration counts

The NLROM-EL method, time-domain numerical simulation, and the proposed method were used to calculate the RMS of the midpoint displacement response of the laminated plates, and the results are shown in Fig. 10. The errors of the NLROM-EL method and the proposed method with respect to the time-domain numerical simulation are given in Fig. 11. Comparisons of the computational time and iteration counts of the NLROM-EL method and the proposed method are given in Fig. 12. It can be observed that the accuracy of this method is better than that of NLROM-EL method in all the cases, and the computational time of the proposed method is almost the same as that of NLROM-EL method.

Next consider the load case where the laminated plates are subjected to a turbulent boundary layer, whose one-sided PSD is expressed as [28]

$$S_{ff}(\boldsymbol{s}_1, \boldsymbol{s}_2, \omega) = \Phi_{ff}(\omega)\Theta(\omega; \boldsymbol{s}_1, \boldsymbol{s}_2) \tag{48}$$

where $\boldsymbol{s} = (x, y)$ is the coordinate vector, Φ_{ff} is the auto PSD of the wall pressure, the geometrical function Θ is expressed as [29]

$$\Theta(\omega; \boldsymbol{s}_1, \boldsymbol{s}_2) = \exp\left(-c_x \left|\frac{\omega\xi_x}{U_c}\right|\right) \exp\left(-c_y \left|\frac{\omega\xi_y}{U_c}\right|\right) \exp\left(\frac{-\mathrm{i}\omega\xi_x}{U_c}\right) \tag{49}$$

where c_x and c_y are constants describing the spatial coherence of the wall pressure field in the longitudinal and transversal directions, respectively, $\xi_x = x_1 - x_2$ and $\xi_y =$

$y_1 - y_2$ represent the distance between two points, and U_c is the convection velocity. The parameters recommended in [28] are adopted

$$c_x = 0.15, \qquad c_y = 0.75, \qquad U_c = 75\text{m/s} \tag{50}$$

The auto PSD of point wall pressure $\Phi_{ff}(\omega)$ is a band-limited white noise covering a frequency range from 10Hz to 1000Hz, and the SPL ranges from 94dB to 142dB, in 6dB increments. The time-domain series simulation of the turbulent boundary layer refers to [30].

The NLROM-EL method, time-domain numerical simulation and the proposed method were used to calculate the RMS of the midpoint displacement response of the laminated plates, and the results are shown in Fig. 13. Fig. 14 gives the error of the NLROM-EL method and the proposed method with respect to the time-domain numerical simulation. Fig. 15 shows comparisons of the computational time and iteration counts of the NLROM-EL method and the proposed method. Finally, Fig. 16 shows the distribution of computational error of the NLROM-EL and the proposed method across the plate. This example is an antisymmetric cross-ply laminated plate subjected to a turbulent boundary layer, where the SPL of the wall pressure is 130dB. It can be observed that the proposed method has a significant advantage in accuracy at any position in the plate.

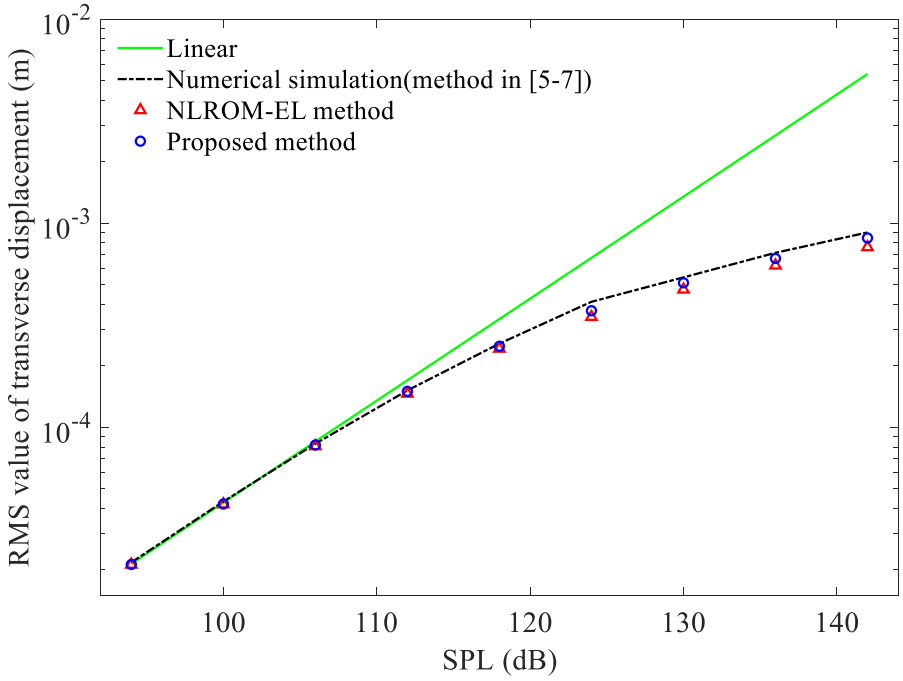

(a) Symmetric cross-ply laminated plate

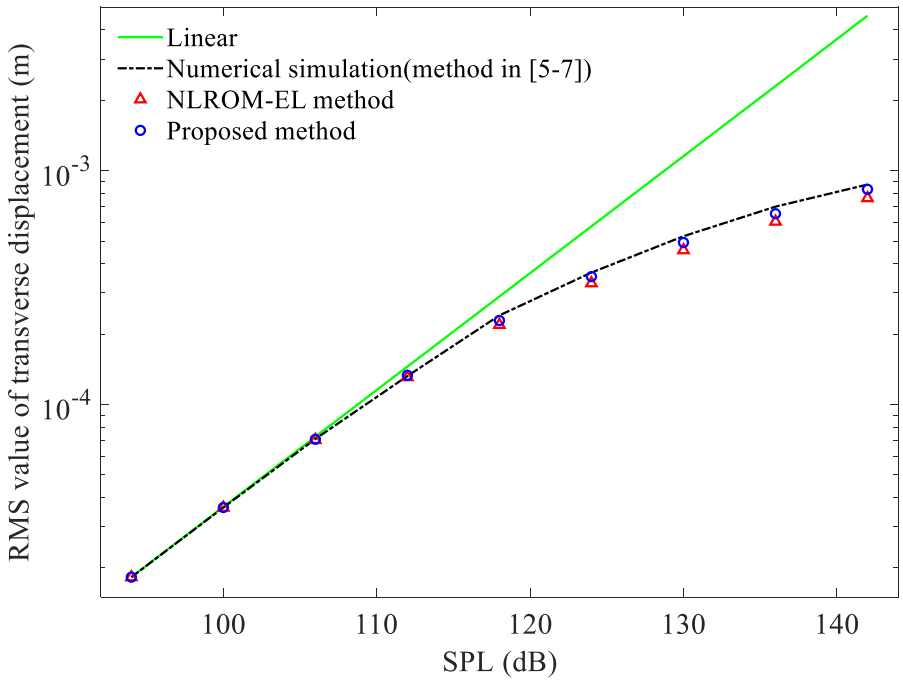

(b) Antisymmetric cross-ply laminated plate

Fig. 13 Comparison of RMS value of midpoint displacement response

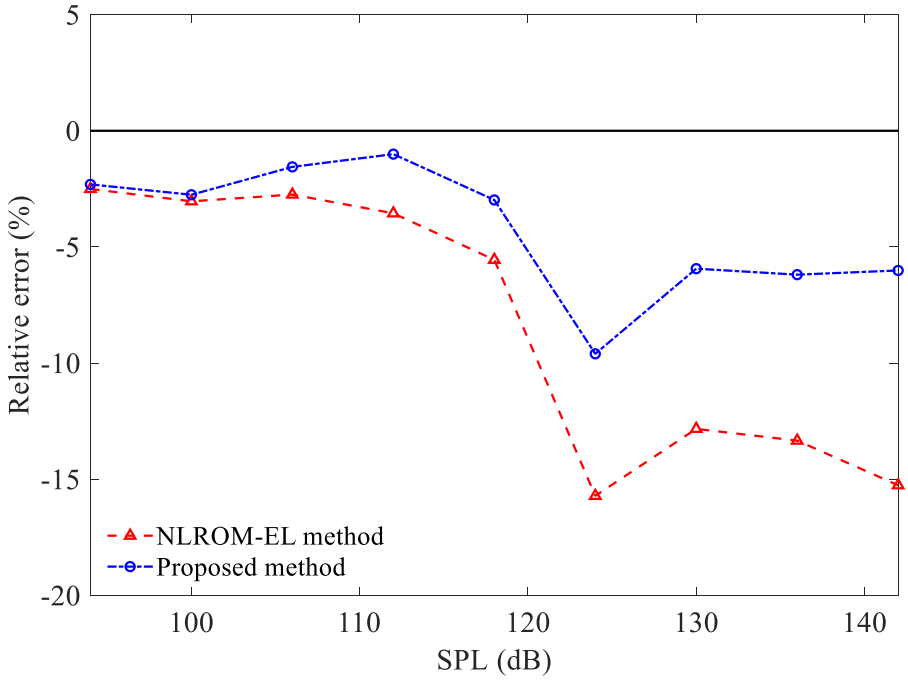

(a) Symmetric cross-ply laminated plate

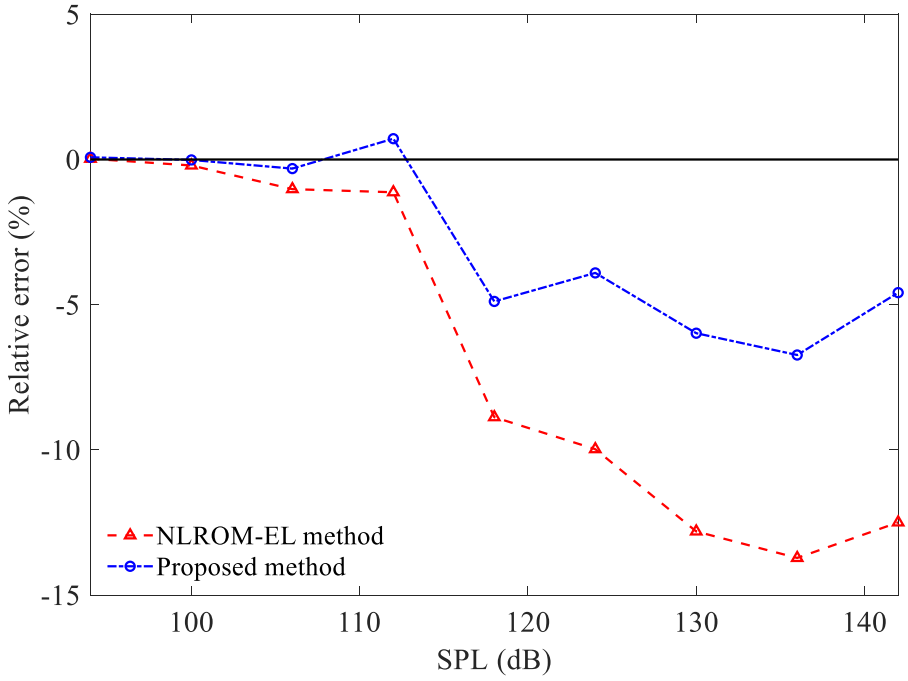

(b) Antisymmetric cross-ply laminated plate

Fig. 14 Comparison of computational error

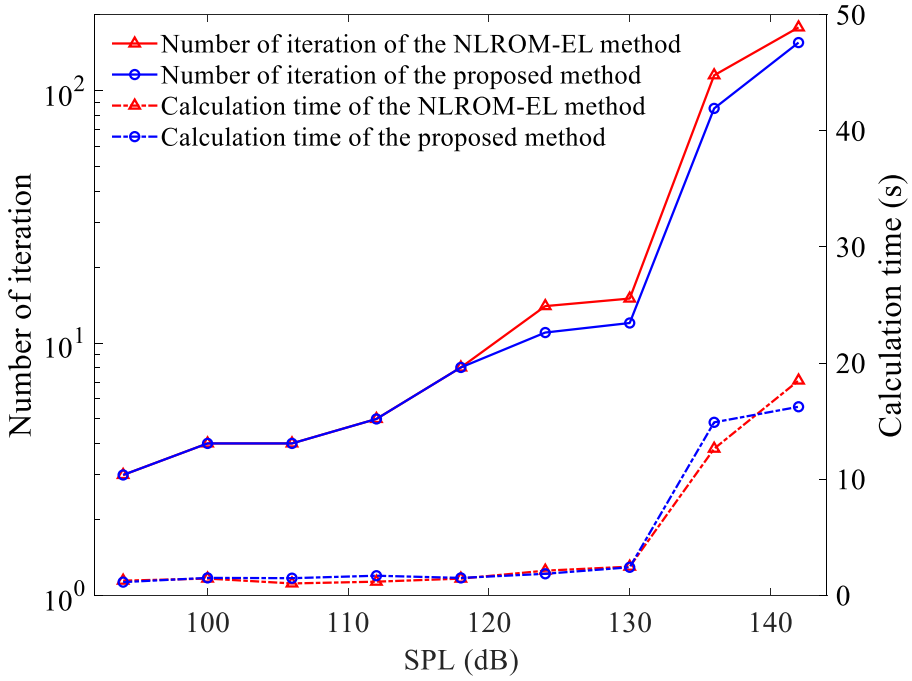

(a) Symmetric cross-ply laminated plate

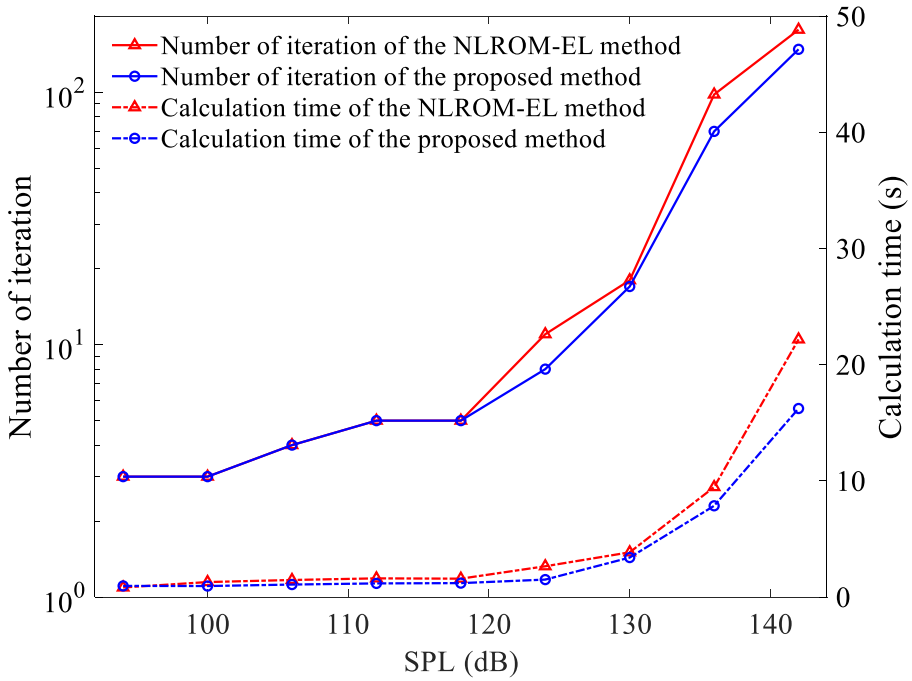

(b) Antisymmetric cross-ply laminated plate

Fig. 15 Comparisons of computational time and iteration counts

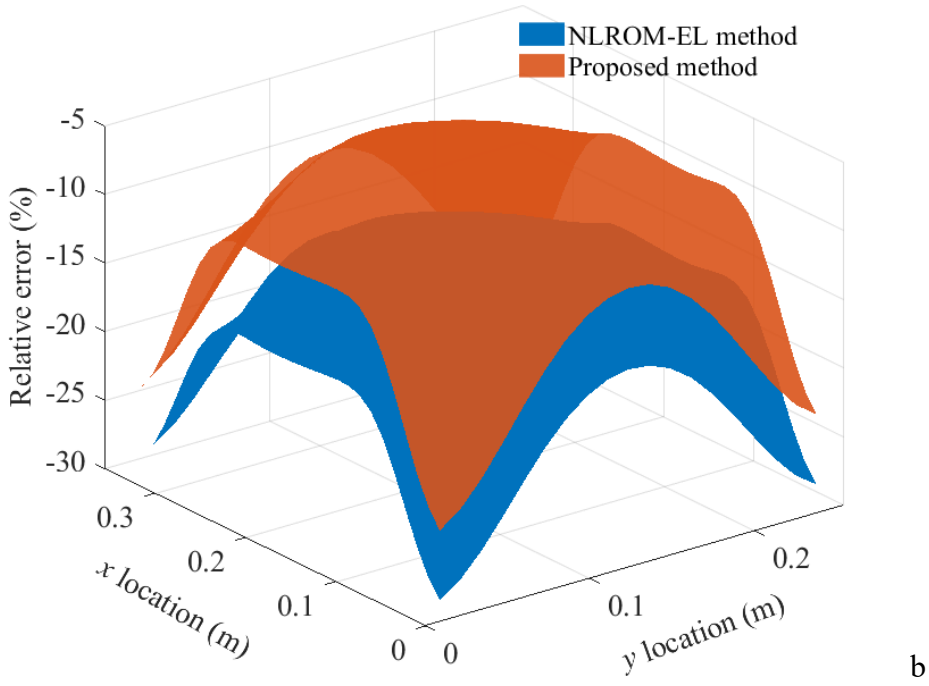

b

Fig. 16 Distribution of computational error in plate

It can be observed from Fig. 9, Fig. 12 and Fig. 15 that when calculating nonlinear random problems, the iteration counts of the NLROM-EL method and the proposed method are very close. At the same time, the proposed method only adds a few basic operations in each iteration calculation, with little additional computational burden, resulting in no increase in the calculation time of the proposed method. It can be concluded from the above examples that the cost of the proposed method is the same as that of the NLROM-EL method. It is worth noting that it took 586s to construct the reduced order model of the laminated plates using the STEP method, while the improved STEP method took 396s, a reduction of 32%. Compared with the EL method, the construction of a reduced order model takes a considerable proportion of the overall computational time, and it is necessary to improve the STEP method. Fig. 6 shows that

the improved STEP method is highly consistent with the NLROM constructed by the STEP method. Further, the cost and results of REL analysis based on the above two methods are given in Table 1. It can be observed that the improved STEP method will hardly affect the iteration convergence and calculation results of nonlinear random problems. Finally, comparisons between the proposed method and the NLROM-EL method are given in Table 2.

6 Conclusions

In this paper, the STEP method is improved by the symmetry relationship of nonlinear stiffness coefficients, and an EL method based on NLROM techniques and modified by higher-order statistics is proposed to predict the response of geometrically nonlinear structures under random excitation. The nonlinear system is regulated and linearized successively to obtain an EL system considering higher order statistics to capture the nonlinear random response efficiently and accurately. The static examples show that the improved STEP method can effectively reduce the cost of stiffness coefficients on the premise of ensuring the quality of NLROM. Subsequent dynamic examples show that the proposed method has the same iterative convergence and cost as the NLROM-EL method, but significantly improves the computational accuracy of nonlinear random response. It is necessary to further extend the proposed method to vibration systems with asymmetric structure or non-zero mean excitation, since only weak nonlinear systems with zero mean are considered in this paper.

Table 1 Comparisons of cost and results of antisymmetric cross-ply laminated plate under band-limited white noise

SPL	STEP method			Improved STEP method		
	Number of iterations	Calculation time(s)	RMS of midpoint(m)	Number of iterations	Calculation time(s)	RMS of midpoint (m)
106	3	1.630974	3.6665e-05	3	1.595720	3.6664e-05
112	4	2.036782	7.2222e-05	4	1.711190	7.2220e-05
118	5	2.239053	1.3809e-04	5	1.764534	1.3790e-04
124	7	1.834199	2.4624e-04	7	1.896202	2.4619e-04
130	10	2.180997	4.0237e-04	10	2.182879	4.0332e-04
136	15	2.725978	6.1500e-04	13	2.525368	6.1578e-04
142	20	2.725978	9.0320e-04	14	2.605017	9.0254e-04
148	34	6.778507	1.2959e-03	30	5.467464	1.2953e-03
154	23	4.523223	1.8576e-03	25	4.609441	1.8543e-03

Table 2 Comparisons between the proposed method and the NLROM-EL method

	Comparison	Reason/Result
NLROM	The NLROM-EL method uses the STEP method to construct the NLROM, while the improved STEP method is used in the proposed method	The computational cost is reduced by about 30%, and the proportion increases with the increase of the number of reduced modes
Accuracy	Compared with NLROM-EL method, the calculation accuracy of the proposed method is obviously improved	Higher order statistics are introduced to improve the calculation accuracy
Cost	The proposed method has the same cost as NLROM-EL method in iteration calculation	Each iteration adds only a few basic operations
Iteration convergence	The proposed method has the same convergence level as NLROM-EL method	REL has no effect on the convergence of iterative calculation
Application scope	The proposed method has the same application scope as NLROM-EL method, that is, weak nonlinear systems	The proposed method does not introduce new computational assumption

Acknowledgments

The authors are grateful for support under a grant from the National Science Foundation of China (12032008), and the Cardiff University Advanced Chinese Engineering Centre.

References

[1] Mignolet MP, Przekop A, Rizzi SA, Spottswood SM. A review of indirect/non-intrusive reduced order modeling of nonlinear geometric structures. Journal of Sound and Vibration, 2013, 332(10): 2437-2460.

[2] Kaminski MM. The Stochastic Perturbation Method for Computational Mechanics. Chichester: John Wiley and Sons, 2013.

[3] Spencer BF Jr., Bergman LA. On the numerical solution of the Fokker-Planck equation for nonlinear stochastic systems. Nonlinear Dynamics, 1993, 4(4): 357-372.

[4] Risken H, Till F. The Fokker-Planck Equation. Berlin: Springer, 1996.

[5] Rizzi SA, Muravyov AA. Comparison of nonlinear random response using numerical integration and equivalent linearization. Proceedings of the 7th International Conference on Recent Advances in Structural Dynamics, Southampton, 2000: 833-846.

[6] Rizzi SA, Muravyov AA. Equivalent linearization analysis of geometrically nonlinear random vibrations using commercial finite element codes. NASA/TP-2002-211761, NASA Langley Research Center, Virginia, 2002.

[7] Shinozuka M, Wen YK. Monte Carlo solution of nonlinear vibrations. AIAA Journal, 1972, 10(1): 37-40.

[8] Proppe C, Pradlwarter HJ, Schuëller GI. Equivalent linearization and Monte Carlo simulation in stochastic dynamics. Probabilistic Engineering Mechanics, 2003, 18(1): 1-15.

[9] Caughey TK. Equivalent linearization techniques. Journal of the Acoustical Society of America, 1963, 35(11): 1706-1711.

[10] Muravyov AA, Rizzi SA. Determination of nonlinear stiffness with application to

random vibration of geometrically nonlinear structures. Computers and Structures, 2003, 81(15): 1513-1523.

[11] Bernard P. Stochastic linearization: what is available and what is not. Computers and Structures, 1998, 76(1), 9-18.

[12] Robinson JH, Chiang CK, Rizzi SA. Nonlinear random response prediction using MSC/NASTRAN. NASA/TM-109029, NASA Langley Research Center, Virginia, 1993.

[13] Elishakoff I, Andriamasy L, Dolley M. Application and extension of the stochastic linearization by Anh and Di Paola. Acta Mechanica, 2009, 204(1-2): 89-98.

[14] Anh ND, Di Paola M. Some extensions of Gaussian equivalent linearization. Proceedings of the International Conference on Nonlinear Stochastic Dynamics, Hanoi, 1995: 5-16.

[15] Anh ND, Elishakoff I, Hieu NN. Extension of the regulated stochastic linearization to beam vibrations. Probabilistic Engineering Mechanics, 2014, 35: 2-10.

[16] Anh ND, Elishakoff I, Hieu NN. Generalization of Seide's problem by the regulated stochastic linearization technique. Meccanica, 2016, 52(4-5): 1-14.

[17] Mignolet MP, Soize C. Stochastic reduced order models for uncertain geometrically nonlinear dynamical systems. Computer Methods in Applied Mechanics and Engineering, 2008, 197(45-48): 3951-3963.

[18] Rizzi SA, Muravyov AA. Improved equivalent linearization implementation using nonlinear stiffness evaluation. NASA/TM-2001-210838, NASA Langley Research Center, Virginia, 2001.

[19] Yang S, Yang Q. Geometrically nonlinear random vibration responses of laminated plates subjected to acoustic excitation. AIAA Journal, 2018, 56(7): 2827-2839.

[20] Perez R, Matney A, Wang XQ, Mignolet MP. Reduced order model for the geometric nonlinear response of complex structures. Proceedings of the ASME 2012 International Design Engineering Technical Conferences and Computers and Information in Engineering Conference, Chicago, 2012: 599-613.

[21] Givois A, Deü JF, Thomas O. Dynamics of piezoelectric structures with geometric nonlinearities: A non-intrusive reduced order modelling strategy. Computers and Structures, 2021, 253:1-23.

[22] Elishakoff I, Andriamasy L. The tale of stochastic linearization technique: over half a century of progress. In: Elishakoff I, Soize C. Nondeterministic Mechanics. Udine:

Springer, 2012: 115-189.

[23] Langely RS. Stochastic linearisation of geometrically non-linear finite element models. Computers and Structures, 1986, 27(6): 721-727.

[24] Rizzi SA, Przekop A. The effect of basis selection on static and random acoustic response prediction using a nonlinear modal simulation. NASA/TP-2005-213943, NASA Langley Research Center, Virginia, 2005.

[25] Przekop A, Rizzi SA. Nonlinear reduced order random response analysis of structures with shallow curvature. AIAA Journal, 2006, 44(8): 1767-1778.

[26] Kuether RJ, Allen MS, Hollkamp JJ. Modal substructuring of geometrically nonlinear finite element models with interface reduction. AIAA Journal, 2017, 55(5): 1695-1706.

[27] Wijker JJ. Random Vibrations in Spacecraft Structures Design. Springer, Netherlands, 2009.

[28] Durant C, Robert G, Filippi PJT, Mattei PO. Vibroacoustic response of a thin cylindrical shell excited by a turbulent internal flow: comparison between numerical prediction and experimentation. Journal of Sound and Vibration, 2000, 229(5): 1115-1155.

[29] Corcos GM. The structure of the turbulent pressure field in boundary-layer flows. Journal of Fluid Mechanics, 1964, 18(3): 353-378.

[30] Shinozuka M, Jan CM. Digital simulation of random processes and its applications. Journal of Sound and Vibration, 1972, 25(1): 111-128.

Figure Captions

Table Captions